DYNA
http://dyna.medellin.unal.edu.co/

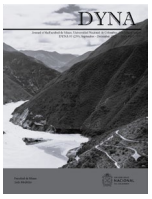

UNIVERSIDAD NACIONAL DE COLOMBIA

Methodology for evaluating the effectiveness of clay inhibition treatments in injection wells: a case study in a colombian field

Jeimy Alejandra Peña-Mateus[a], María Paula Mosquera-González[a], Eduardo Alfredo Gómez-Cepeda [a], Franklin Iván Archer-Martinez [a] & Jaqueline Jaimes-Barajas [b]

[a] *Laboratorio de Diagnóstico de Pozos, Escuela de Ingeniería de Petróleos, Universidad Industrial de Santander, Bucaramanga, Colombia. jeimy2218452@correo.uis.edu.co, eip.gestorproyectos3@uis.edu.co, labpetrofisicos@uis.edu.co, franklin.archer.ve@gmail.com*
[b] *SierraCol Energy, Bogotá, Colombia. yacqueline_jaimes@sierracol.com*

Received: June 24th, 2025. Received in revised form: August 13th, 2025. Accepted: August 22nd, 2025.

Abstract
In the mature fields of the Middle Magdalena Valley Basin (VMM), high water production and limited disposal capacity pose operational challenges, particularly due to the declining efficiency of injection wells. The operating company, in collaboration with the Industrial University of Santander (UIS), evaluated the use of chemical inhibitors based on the hypothesis that injectivity loss was caused by clay swelling. However, laboratory tests ruled out swelling and identified fines of migration as a potential limiting factor. To validate these findings, a field evaluation methodology was developed, involving real-time monitoring of injection rates and pressure variations using different concentrations of chemical product. The results confirmed that the injected chemical product does not significantly improve injectivity, leading to the conclusion that discontinuing the injection of the inhibitor is the best option to optimize field operations from a cost-benefit perspective.

Keywords: mature fields; injectivity; clays; inhibitors; swelling; fines migration; laboratory testing; field methodology; water injection wells.

Metodología para la evaluación de la eficacia de tratamientos de inhibición de arcilla en pozos inyectores: caso de estudio en un campo colombiano

Resumen
En los campos maduros de la Cuenca del Valle Medio del Magdalena (VMM), la alta producción de agua y la limitada capacidad de disposición generan desafíos operacionales, especialmente por la pérdida de eficiencia de los pozos inyectores. La empresa operadora, en conjunto con la Universidad Industrial de Santander (UIS), evaluó el uso de inhibidores químicos ante la hipótesis de que la disminución de inyectividad se debía al hinchamiento de arcillas. Sin embargo, las pruebas de laboratorio descartaron este fenómeno e identificaron la migración de finos como un factor relevante. Para validar estos resultados, se diseñó una metodología de evaluación en campo, monitoreando en tiempo real la tasa de inyección y las variaciones de presión con diferentes concentraciones del producto químico. Los resultados corroboraron que el inhibidor de hinchamiento inyectado no mejora significativamente la inyectividad, lo que lleva a la conclusión de que retirar la inyección del inhibidor es la mejor opción para optimizar la operación desde el punto de vista costo-beneficio.

Palabras clave: campos maduros; inyectividad; arcillas; inhibidores, hinchamiento; migración de finos; pruebas de laboratorio; metodología de campo; pozos inyectores de agua.

1 Introduction

In Colombia's mature oil fields, efficient produced water management poses a critical challenge for the petroleum industry. With an average water-to-oil ratio of 13:1, the handling of this large volume of water has become both an operational and environmental priority [12]. This issue is especially critical in fields within the Middle Magdalena

How to cite: Peña-Mateus, J.A., Mosquera-González, M.P., Gómez-Cepeda, E.A., Archer-Martinez, F.I., and Jaimes-Barajas, J., Methodology for evaluating the effectiveness of clay inhibition treatments in injection wells: a case study in a colombian field. DYNA, (92)239, pp. 38-48, October - December, 2025.

Valley Basin (VMM), where existing infrastructure inadequate to meet the growing demands for produced water treatment and disposal, making reinjection the primary management strategy [14]. However, the effectiveness of injection wells, crucial for maintaining sustainable production, tends to decline over time due to reduced injectivity. One hypothesis attributes this reduction in reinjection efficiency to clay hydration and swelling. In response, chemical solutions involving swelling inhibitors have been investigated as a potential mitigation strategy.

Clay swelling poses a significant challenge in the oil and gas industry, particularly in reservoirs containing expandable clay minerals [25]. Water injection, a widely adopted secondary oil recovery method [24], can trigger this undesirable phenomenon, often with serious consequences [22]. As a foreign fluid, injection water may be geochemically incompatible with the reservoir rock, potentially inducing clay swelling. The primary outcome is formation damage, leading to reduced water injectivity [17,24].

To mitigate clay swelling during water injection operations, laboratory evaluations are essential to understand the mechanisms involved and to develop strategies for controlling formation damage [11]. This study employs a practical and comprehensive experimental approach consisting of three stages aimed at assessing the effectiveness of various concentrations of a commercial swelling inhibitor. Additionally, a field-based methodology is presented to evaluate the performance of clay swelling inhibition treatments in injection wells within the VMM. The inhibitor's impact on well injectivity is assessed through field-monitored tests by analyzing changes in instantaneous injection rates and pressure behavior over time.

1.1 Swelling Phenomenon

Clay minerals are crystalline hydrated sheet silicates composed of tetrahedral silicate layers connected to octahedral layers [13]. Typically fine-grained, they can form plastic masses when mixed with water [15]. They are classified into four main groups: Kaolinite, Chlorite, Smectite, and Illite. Mixed-layer clays result from combinations of these groups. Kaolinite forms stacked plates that disintegrate and migrate, blocking pores. Chlorite precipitates gelatinous iron hydroxides in acidic or oxygenated conditions. Smectite, with irregular expandable sheets, is highly water-sensitive and reduces microporosity and permeability. Illite, with elongated spines, can transform into expandable clays through potassium leaching. Mixed-layer clays disintegrate into clumps that bridge pores, reducing permeability [15].

Swelling clays have a crystalline structure with an octahedral Al-OH (or Fe-OH or Mg-OH) layer sandwiched between two tetrahedral Si-O layers. Due to cation substitution, these layers have a charge deficiency balanced by exchangeable interlayer cations [13]. These cations, such as Na^+, K^+, or Ca^{2+}, influence the interlayer spacing depending on their nature, the solution composition, and the clay's structural characteristics. Clay swelling results from increased interlayer spacing when these cations hydrate in water [13,17,26]. Smectite shows the highest swelling due to its weak intercrystalline bonds that easily admit water or polar substances [16].

There are two types of swelling: crystalline and osmotic [4,20,25]. Crystalline swelling, described by Zhou et al. (1996), occurs in concentrated brines or in the presence of multivalent cations, forming molecular water layers and causing minimal swelling. Osmotic swelling, induced by dilute solutions or high sodium concentrations, creates electric double layers, leading to greater swelling and formation damage.

To mitigate swelling, inhibitors such as inorganic salts (e.g., KCl, NH_4Cl) and organic compounds (e.g., polymers) are used. It is important to distinguish between chemicals that inhibit clay hydration and those that promote clay stability: the former limit water penetration, while the latter prevent both swelling and fine migration [7].

1.2 Study area

This study was conducted in a field located within the VMM, a 32,949 km² area situated between Colombia's Central and Eastern Cordilleras. The VMM is one of the country's most prolific hydrocarbon basins, with 51 oil fields discovered in Cenozoic sediments. Exploration has primarily focused on structural traps within the Cenozoic sequence, while stratigraphic traps remain underexplored. The Cretaceous sequence includes marine and transitional deposits, whereas Cenozoic rocks are predominantly continental.

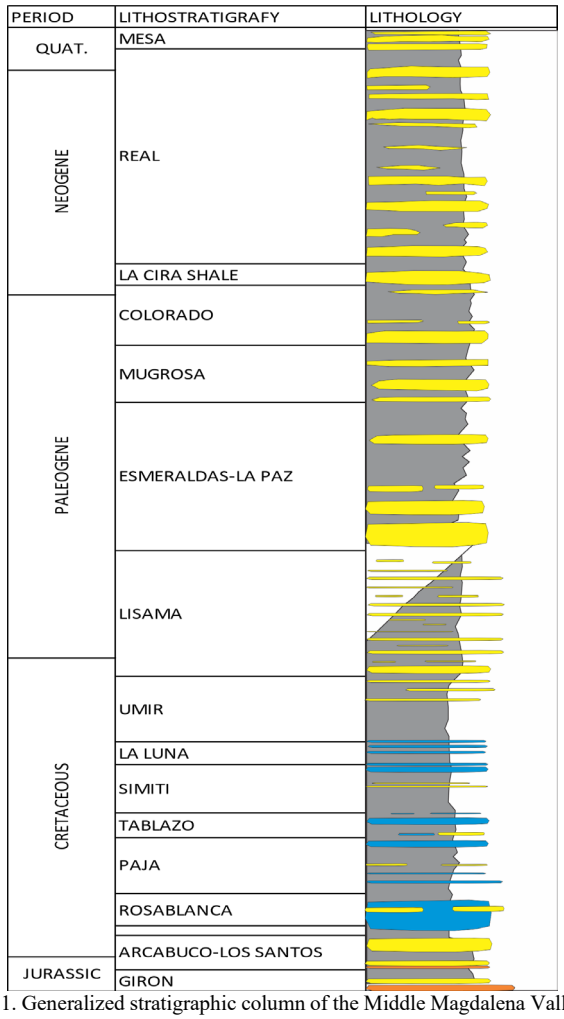

Figure 1. Generalized stratigraphic column of the Middle Magdalena Valley Basin (VMM).
Source: Own elaboration.

The main source rocks in the basin are the La Luna, Simití, and Tablazo formations (Fig. 1). Hydrocarbon migration occurs along Eocene unconformities and faults. Reservoirs consist mainly of high-porosity, high-permeability Cenozoic sandstones, sealed by marine shales and continental claystones. The basin holds significant exploration potential, particularly in Cretaceous carbonates and Upper Miocene–Eocene stratigraphic traps, with estimated resources ranging from 600 to 8,000 million barrels. Seismic and geological studies have identified prospective structures, while geochemical analyses indicate biodegraded oils with variable maturity [23].

2 Methodology

The study methodology is divided into two phases: an experimental laboratory-scale phase and a field evaluation phase.

2.1 Experimental laboratory-scale phase

To address operational issues related to low injectivity in the study field's sandstone formations, an experimental evaluation was conducted to assess the performance of a clay swelling inhibitor across various lithological samples. The methodology, outlined in Fig. 2, includes basic characterization of both fluid and rock samples, along with fluid-fluid and rock-fluid interaction tests under static and dynamic conditions.

2.2 Materials

2.2.1 Trench samples and core samples

The availability of core or plug samples is often limited during experimental evaluations. As an alternative, trench samples—rock cuttings taken directly from the intervals of the reservoir under study—were used to assess the performance of the clay swelling inhibitor. While trench samples do not characterize the entire reservoir and inherently carry some degree of uncertainty, they are considered representative of the specific zones where injectivity loss was observed. In this study, three trench samples (Table 1), each averaging 500 grams, were analyzed. Additionally, highly reactive commercial clays with known properties were included to complement the evaluation objectives.

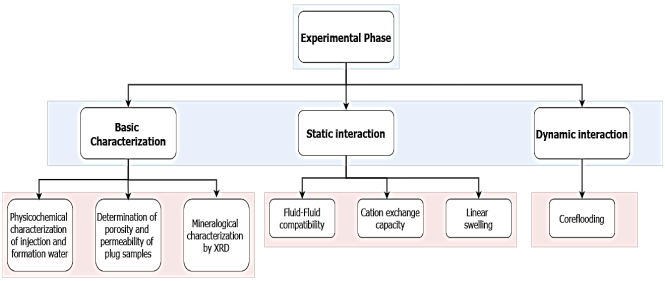

Figure 2. Laboratory methodology workflow diagram.
Source: Own elaboration.

Table 1.
Trench samples used in the study

Sample Number	Identification	Depth (ft)
1	Trench Sample 1X	1399,4
2	Trench Sample 2X	1407,7
3	Trench Sample 3X (Reactive Clays)	1362,90

Source: Own elaboration.

Table 2.
Petrophysical properties of core samples used in the study

ID	Depth(ft)	Porosity (%)	Kair (nD)	Pore Volume (cc)
Core 1X	1399.4	31.15	930	19.37
Core 3X	1362.9	24.53	19	14.8

Source: Own elaboration.

On the other hand, two plug samples from the studied formation were used in displacement tests. The core samples were properly preserved and cleaned according to an adaptation of API RP 40 (1998) standards. Each sample measured 1 inch in diameter and 2.2 inches in length. Their petrophysical properties are summarized in Table 2.

2.2.2 Clay characterization

X-ray diffraction (XRD) was used to determine the mineralogical composition of the trench samples, with emphasis on identifying and estimating the content of expandable clay minerals. As shown in the Fig. 3, all samples exhibit a high proportion of kaolinite, a non-expandable clay mineral (green). In contrast, Sample 3X contains approximately 1.18%, a moderately expandable clay. These results indicate that Sample 3X includes swelling-prone minerals with potential for clay reactivity. The study focuses on the swelling and hydration behavior of the clay mineral fraction, as these mechanisms are directly linked to formation damage, rather than on identifying specific exchangeable cations.

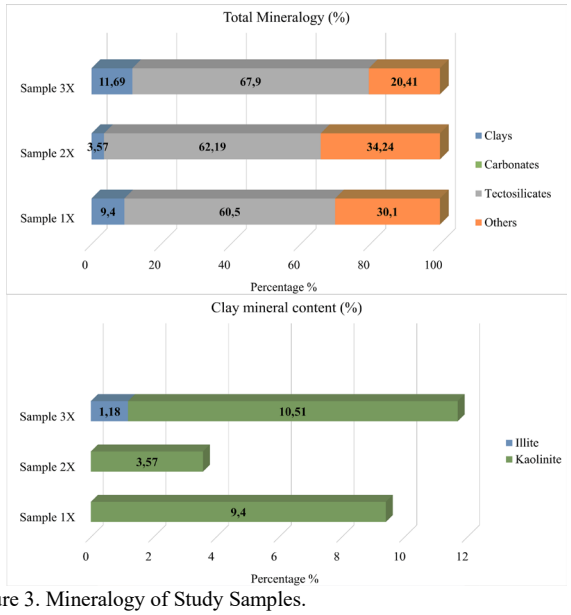

Figure 3. Mineralogy of Study Samples.
Source: Own elaboration.

Table 3.
Properties of the brines used in the study

Property	Formation Water	Injection Water
Conductivity (mS/cm)	25.93	26.32
Total Dissolved Solids - TDS (g/L)	17.74	16.67
Alkalinity (mg$CaCO_3$/L)	806.67	646.67
pH	7.27	6.71

Source: Own elaboration.

Table 4.
Evaluation matrix

	FW	IW	FC	CSI
FW	N/A	x	x	x
IW	N/A	N/A	x	x
FC	N/A	N/A	N/A	x
CSI	N/A	N/A	N/A	N/A

Note: Mixing ratios of 20/80, 50/50, and 80/20 were evaluated for each fluid pair. "N/A" indicates that the evaluation was not applied to those combinations. FW: Formation Water, IW: Injection Water, FC: Formation Crude, CSI: Clay Swelling Inhibitor
Source: Own elaboration.

2.2.3 Fluids

The fluids used in the tests included synthetic brines formulated based on the chemical composition of field fluids (Table 3), formation crude oil, and a commercial clay swelling inhibitor. Injection water was used as the base for inhibitor solutions in static and dynamic tests.

2.3 Compatibility test

Fluid-fluid incompatibilities are a key cause of formation damage [9]. Thus, the first step in the experimental evaluation is to assess the compatibility between the injection fluid (brine with inhibitor) and reservoir fluids (formation water and crude oil). Mixtures at ratios of 50:50, 20:80, and 80:20 (Table 4) were prepared (100 mL total) and stored at 50°C to simulate reservoir conditions. Observations for precipitates, phase separation, turbidity, emulsions, or other anomalies were made at 0.5, 1, 2, 4, 6, and 24 hours, with deviations recorded to determine compatibility.

2.4 Evaluation of clay-water interaction in the presence of inhibitors

2.4.1 Cation Exchange Capacity (CEC)

The CEC represents the total exchangeable ions on clay surfaces in contact with aqueous solutions and is measured in meq/100 g [19]. It is commonly used to assess clay swelling potential [1,3,8,10]. In this study, CEC was estimated using the methylene blue capacity test following API RP 13I [5]. This test involves adding methylene blue solution to a mixture of injection water, inhibitor, and clay, pretreated with hydrogen peroxide and acidified, until saturation is indicated by a dye "halo" forming around a drop of the suspension on filter paper, helping to corroborate clay reactivity related to swelling and hydration.

2.4.2 Linear swelling

Linear swelling tests, used in previous studies [1,7,18,21], evaluate swelling potential without requiring core samples. Trench samples were sieved (200 mesh) and compressed hydraulically (20 g, 10,000 psi, 30 min) into small cylinders. These were submerged in test fluids, and a linear swell meter recorded vertical expansion over time. Swelling rate (%) was calculated as the swollen height relative to the initial height.

2.4.3 Core displacement

Core injection experiments have been used to characterize the effect of clay swelling on reservoir quality [17,25,24,2]. These experiments consist of injecting one or more fluids through a core plug to measure pressure drop and, consequently, calculate permeability using Darcy's law and its constraints.

All experiments were conducted in Hassler-type core holders. Nitrile rubber was used as sleeve material. Confining pressure was applied with distilled water using a Ruska-type pump, while the backpressure valve was controlled with nitrogen. In each experiment, the core holder was mounted horizontally, allowing fluid injection from either end. A valve system enabled reversing the flow direction without removing the core.

The system used a positive displacement pump to inject fluids and four electrically controlled valves to regulate flow and fluid type. Differential diaphragm-type pressure transducers were used to measure the pressure drop across the core. The operating conditions for all experiments are listed in Table 5.

The core injection protocol serves as a guide for executing the process, detailing the type of fluid to inject, the number of pore volumes to flood, the variable to determine, the injection direction, and the injection rate. Core displacements were carried out on two specific samples: Sample 1X and Sample 3X. These evaluations focused not only on analyzing the behavior and properties of the samples within a porous medium but also on assessing their sensitivity to the clay swelling inhibitor. This additional evaluation provided insight into how the samples respond to the presence of the inhibitor and its impact on their behavior and performance.

Based on the results of static tests and the established displacement protocols for evaluating clay swelling, a specific protocol was developed for each sample, ensuring compliance with the necessary technical specifications for fluid evaluation. Sample 1X was first vacuum-saturated and mounted in the displacement equipment to determine effective porosity. Formation brine was then injected until 100 stable pore volumes were reached at a rate of 0.1 cc/min, allowing for the determination of absolute permeability to water. Subsequently, injection brine was displaced under the same conditions to evaluate effective permeability, followed by the determination of the sample's critical rate.

Table 5.
Operating parameters for core injection experiments

Parameter	Value
Temperature	50 °C
Reservoir Pressure	500 psi
Injection Rate	0.15 cm³/min (Verified at 0.1 cm³/min and 0.05 cm³/min)
Confining Pressure	1200 psi

Source: Own elaboration.

Table 6.
Wells selected based on historical injection performance for field evaluation.

Lithostratigraphic Unit	Injector Well
U1	A
U1	B
U2	C
U2	D

Source: Own elaboration.

For Sample 3X, after vacuum saturation and the assessment of absolute permeability, the critical rate was determined before injecting brine with the clay swelling inhibitor at concentrations of 0.6 GPT, 0.4 GPT, and 0.2 GPT. In each stage, 100 stable pore volumes were reached at 0.1 cc/min to evaluate effective permeability with each inhibitor concentration, followed by intermediate critical rate determinations. Finally, injection brine without an inhibitor was displaced to obtain the final effective permeability, concluding with a final assessment of the sample's critical rate.

2.5 Field evaluation phase

After completing the experimental phase to assess the performance of the commercial clay swelling inhibitor at the laboratory scale, the injection history at the field scale was analyzed. This historical data was used to select candidate wells for evaluation, aiming to analyze injectivity behavior by varying the concentration of the clay swelling inhibitor to assess its effectiveness in the field.

The historical injection performance of the field wells was assessed based on the following activities, using data from the candidate wells with the following characteristics: Injection profiles and injection history, well logs, mechanical diagram and injection configuration, history of well interventions, inhibitor dosage history over time.

Based on this information, a correlation was established between well completion, petrophysics, and injectivity for each candidate well. Additionally, the variation in injectivity over time was correlated with the intervention history, as shown in Figs. 4 and 5.

2.5.1 Injector well A

Fig. 4 shows that the Injector Well A, has good sand quality across all perforated intervals; however, the lower sands, despite their favorable properties, show poor fluid intake, likely due to formation damage during drilling or completion. As shown in Fig. 5, the well's injectivity is mainly affected by mechanical failures, limiting the evaluation of the inhibitor's effectiveness. Consequently, field tests with inhibitor concentration variations are recommended to assess formation sensitivity. Based on historical injection performance, four injector wells from two lithostratigraphic units were selected for field evaluation (Table 6).

For the execution of the field test, certain theoretical considerations are considered, utilizing data that is typically recorded with relative ease. These data allow the identification of changes in the injection capacity of the wells as the injection process progresses, with variations in the inhibitor concentration.

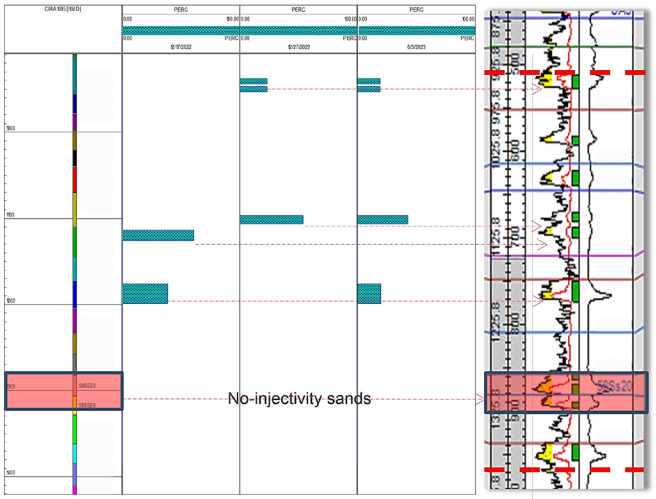

Figure 4. Correlation between the injection profile and the petrophysical properties of the Injector Well A.
Source: Own elaboration.

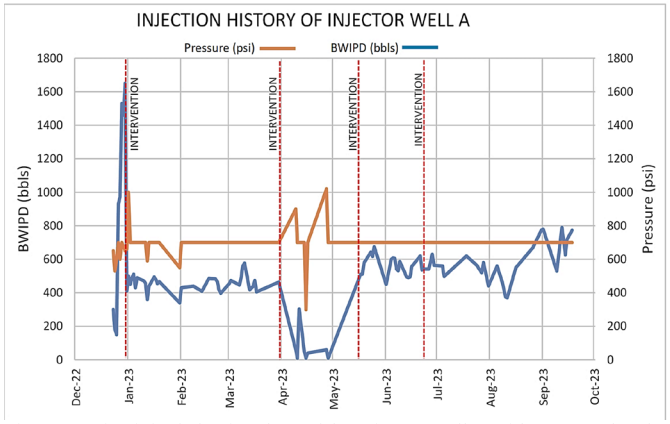

Figure 5. Injectivity behavior chart of the Injector Well A with events related to injection valve changes.
Source: Own elaboration.

The required data for applying this method are: Water injection rate, Surface injection pressure over time, Inhibitor concentration.

With the selected wells, the field test is carried out, and the corresponding variables are interpreted, following the operational procedure illustrated in Fig. 6.

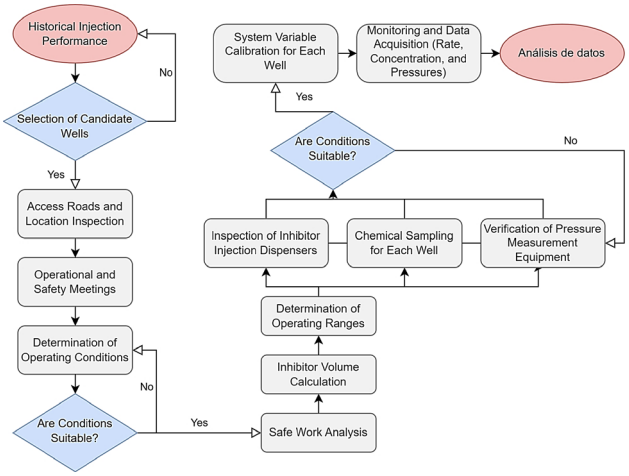

Figure 6. Field methodology workflow diagram.
Source: Own elaboration.

The method is based on Darcy's radial flow equation, expressed as follows:

$$q = \frac{0{,}00708 * k_w * h}{\mu_w ln\frac{r_e}{r_w}}(p_{iwf} - \bar{p}) \quad (1)$$

Where: p_{iwf} = Injection pressure at the formation face (psi), r_e = External drainage radius (ft), r_w = Well radius (ft), k_w = Water permeability (absolute) (mD), h = Formation thickness (ft), $\underline{p}$ = Average reservoir pressure around the injector well (psia), μ_w = Fluid viscosity (cP).

The p_{iwf} an be expressed as:

$$p_{iwf} = p_{tf} + \Delta p_{tw} \quad (2)$$

Where: p_{tf} = Injection pressure at the wellhead (psi), Δp_{tw} = Pressure of the water column at the sand face (psi).

The change in $\underline{p}$ over time is negligible compared to the change in injection pressure p_{iwf}. This pressure must be referenced at the same level as Δp_{tw}. Therefore, simplifying:

$$\Delta p_{tw} = Water\ gradient * D \quad (3)$$

Where D is the reference depth used, in feet (which must be calculated beforehand). The reference depth can typically be selected as the top of the sand or the midpoint of the perforations. The accumulated volume of injected water can be expressed as:

$$W_i = \int_0^t q\ dt = \frac{0{,}00708 * k_w * h}{\mu_w ln\frac{r_e}{r_w}} \int_0^t (p_{iwf} - \bar{p})\ dt \quad (4)$$

Simplifying and grouping all terms:

$$\sum \Delta\,(p_{iwf} - \bar{p})\,\Delta t \cong m_H W_i \quad (5)$$

Where:

$$m_H = \frac{142\ \mu_w ln\frac{r_e}{r_w}}{k_w h} \quad (6)$$

Based on this, a design matrix is created using the inhibitor concentrations and injection rates to be evaluated:

$$\boldsymbol{Qi\ vs\ \varphi i} \quad (7)$$

Where: φi =Variation of inhibitor concentration, Qi = Variation of injection rates.

3 Results

3.1 Laboratory results

3.1.1 Fluid-Fluid Interaction (Compatibility Tests)

Overall, good compatibility was observed between the formation fluids, injection water, and the clay swelling inhibitor, with no evidence of sedimentation, crystallization, film formation, or emulsion development (Fig. 7).

3.1.2 Rock-fluid interaction

CEC: When performing the cation exchange test on rock samples 1X and 2X provided by the company, an immediate reaction was observed upon adding 1 ml of methylene blue. This rapid saturation indicates that the clays are non-reactive,

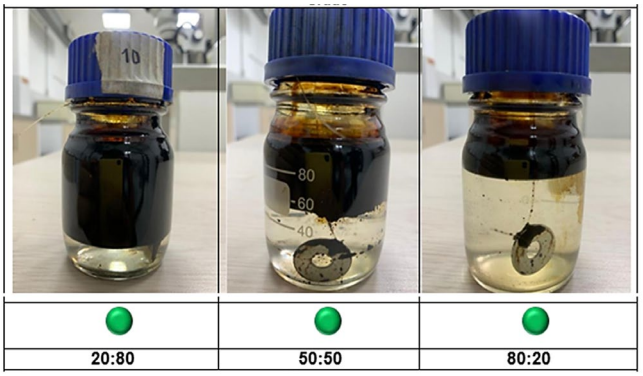

Figure 7. Compatibility Test (Formation Water + Injection Water (0.8 GPT Inhibitor) + Crude Oil).
Source: Own elaboration.

Table 7.
Summary of cation exchange tests - Sample 3X (Reactive Sample)

Evaluated Fluid	Methylene Blue Volume (ml)
Formation Water (FW)	4
Injection Water (IW)	5
IW + IH 0.8 GPT	4
IW + IH 0.6 GPT	4
IW + IH 0.4 GPT	5
IW + IH 0.2 GPT	5

Source: Own elaboration.

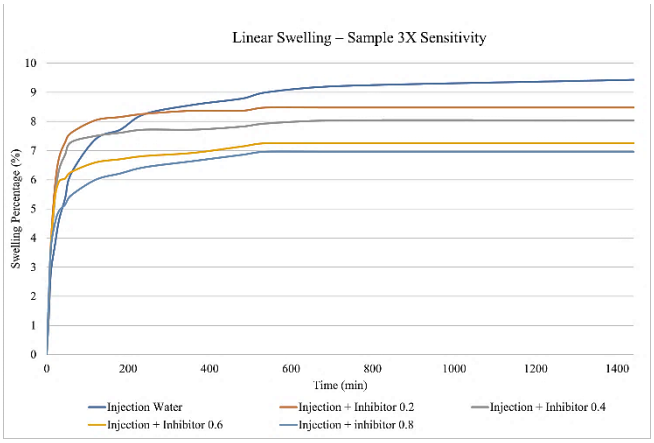

Figure 8. Linear swelling curves for Sample 3X – Swelling inhibitor sensitivity analysis.
Source: Own elaboration.

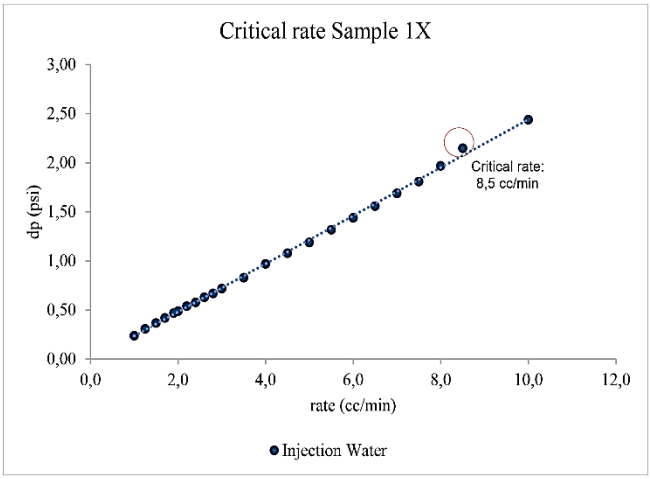

Figure 9. Critical rate estimation with injection water.
Source: Own elaboration.

Table 8.
Linear swelling percentages for samples 1X, 2X, and 3X – sensitivity analysis

Swelling Percentage (24 hours)	AF	AI	AI + IH 0.2GPT	AI + IH 0.4GPT	AI + IH 0.6GPT	AI + IH 0.8GPT
Sample 1X	1.96%	5.54%	3.58%	3.11%	3.04%	0.0%
Sample 2X	3.26%	4.45%	4.43%	4.32%	4.14%	0.0%
Sample 3X	6.16%	9.43%	8.47%	8.03%	7.25%	6.96%

Source: Own elaboration.

Table 9.
Pressure differentials obtained for the recorded flow rates – Sample 1X

Injection Rate (cc/min)	Avg. Δp (psi) – FW	Avg. Δp (psi) – IW
1.0	0.24	0.24
1.3	0.31	0.31
1.5	0.36	0.36

Source: Own elaboration.

Table 10.
Permeability and Critical Rate Evaluated for Sample 3X

Evaluated Fluid	Permeability (mD)	Critical Rate (cc/min)
FW	K_abs = 0.46	0.6
IW	K_winy = 0.42	0.65
IW + IH 0.2 GPT	K_winy0.2 = 0.47	0.6
IW + IH 0.4 GPT	K_winy0.4 = 0.52	0.95
IW + IH 0.6 GPT	K_winy0.6 = 0.45	0.8

Source: Own elaboration.

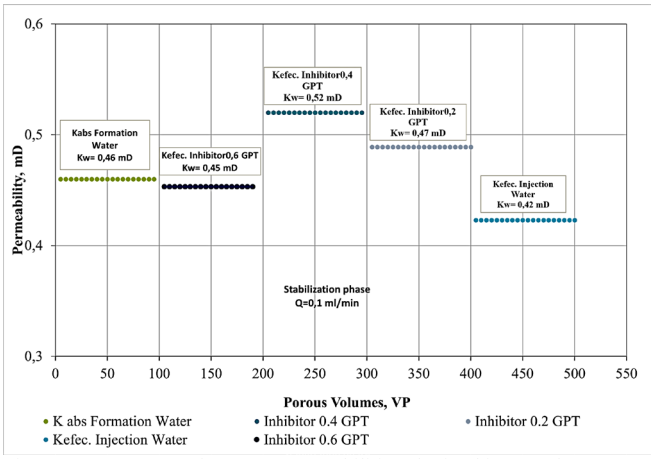

Figure 10. Summary of average permeabilities obtained in Sample 3X
Source: Own elaboration.

which is directly associated with a low swelling potential.

On the other hand, Table 7 presents the results of the cation exchange test performed on rock sample 3X, were the clay's sensitivity to changes in inhibitor concentration was evaluated.

Linear Swelling: To assess the effect of inhibitor concentration on clay swelling, concentrations ranging from 0.2 to 0.8 GPT were tested in 0.2 GPT increments. Table 8 summarizes the results, while Fig. 8 displays the swelling behavior of Sample 3X.

3.1.3 Displacement of synthetic formation brine and injection brine

As proposed, the injection of formation water into sample 1X was initiated, obtaining the results shown in Table 9.

The absolute permeability to water (k_{abs}) and the average permeability to injection water (k_{winy}) were determined based on the experimental data:

$$k_{abs} = 268{,}7\ mD$$

$$k_{winy} = 268{,}3\ mD$$

Critical Rate Estimation: Following the measurement of effective permeability to injection water, the critical rate was determined by gradually increasing the flow rate from 1 cc/min until a noticeable change in pressure differential indicated permeability alteration. For Sample 1X, this inflection point is shown in Fig. 9, which presents the pressure differential as a function of injection rate.

In the displacement test on Sample 3X, which contains a representative amount of reactive clays, no significant permeability changes were observed during the inhibitor sensitivity evaluation. Fig. 10 and Table 10 present the

permeability results and critical rate determined using formation and injection water, with and without inhibitor. The findings highlight the influence of inhibitor concentration on the minimum required injection rate.

An 8.70% reduction in permeability was recorded between formation water and injection water without an inhibitor. However, in line with the results of static tests (CEC and linear swelling), permeability increases when injecting the brine formulated with 0.4 GPT of the commercial clay swelling inhibitor. This phenomenon could be attributed to inhibitor adsorption, suggesting an improvement in the efficiency of the clay inhibition treatment.

3.2 Field results

Based on the results obtained from the static and dynamic laboratory tests, where no significant variations were observed in the injection rates of the brines in the core samples (1X, 2X, and 3X) with respect to the use of a commercial inhibitor at different concentrations, a field test was conducted to validate this behavior. The test aimed to assess the sensitivity of the commercial inhibitor's performance by varying its concentration (0.2, 0.4, and 0.6 GPT) at different water injection rates (700, 900, 1000, 1100, and 1200 bbl/day) in four wells (A, B, C, and D) from two lithostratigraphic units (U1 and U2). The objective was to observe the instantaneous pressure variations over time.

The following section presents the data collected from the evaluated wells, focusing on the sensitivity assessment of injector well A.

4 Results analysis

Once the field test was conducted, laboratory results were confirmed to be consistent. The analysis of instantaneous injection rate variations revealed the inhibitor's sensitivity to pressure changes across different injection scenarios: low, medium, and high.

Low rates (≤700 bbls/d): Inhibitor concentration had minimal impact on injectivity. In Well A, lower pressures were observed with reduced inhibitor dosing, while in Well C, a high concentration (6 GPT) caused an unfavorable pressure increase and reduced injectivity (Fig. 12). At medium rates (900-1100 bbls/d): No significant differences in injectivity were observed. At high rates (≥ 1200 bbls/d and > 1000 bbls/d): A probable migration of fines was considered, leading to a sudden pressure increase, with no evidence that the inhibitor prevented this condition at any evaluated concentration.

In summary, the evaluated injection wells showed low or no sensitivity of injectivity to inhibitor concentration, except in specific cases at high concentrations possibly related to fines migration. A statistical analysis of field data (injection rate, pressure, and inhibitor concentration) was conducted using scatter plots to identify patterns and correlations, and box plots and dot plots to assess pressure variability and distribution at different inhibitor concentrations.

4.1 Sensitivity of injector well A

According to the scatter plot data for Injector Well A (Fig. 11), pressure is directly influenced by the injection rate. However, three distinct scenarios regarding the inhibitor's influence can be identified: First scenario: At low injection rates (≤ 700 bbls/d), inhibitor concentration variations do not significantly affect well injectivity. However, at low inhibitor concentrations (≤ 0.2 GPT, only in Injector Well A), lower pressure values were reported. Second scenario: At intermediate rates (900-1100 bbls/d), no significant differences in injectivity were observed. Third scenario: At high rates (≥ 1200 bbls/d), sudden pressure increases were observed, presumably due to fines migration. However, there is no evidence that the inhibitor improves this condition at any evaluated concentration. To complement the above, Fig. 11, showing box-and-whisker plots, illustrates lower variability and greater consistency in pressure data when lower inhibitor concentrations are used, whereas higher inhibitor concentrations lead to greater pressure variability.

Considering the possible scenarios, a pressure estimation at 0 GPT concentration and a rate of 700 bbl/day was performed using a machine learning analysis with minimization models to determine the ideal rate and concentration values that minimize injection pressure. Additionally, pressure was projected for the extreme considered concentrations (0.2 GPT and 0.6 GPT), where it was observed that at lower concentrations (≤ 0.2 GPT), the average pressure obtained was equivalent to that reached with higher concentrations.

This demonstrates the possibility of operating the well at a lower inhibitor concentration (≤ 0.2 GPT) at injection rates equal to or lower than 700 bbl/day, ensuring efficient performance both operationally and cost-wise (Table 11).

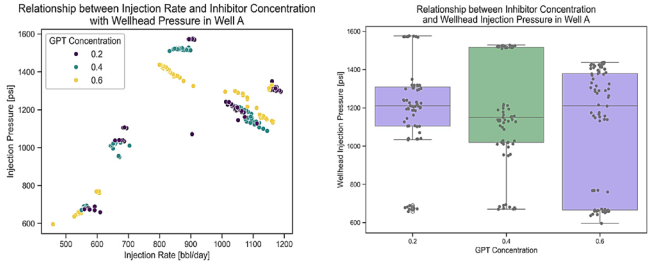

Figure 11. Scatter plot of pressure data in relation to injection rate and inhibitor concentration in the Injector Well A and Pressure variability and dispersion for each concentration used in Injector Well A.
Source: Own elaboration.

Table 11.
Prediction of pressure in Injector Well A using machine learning methods:

Injection Rate [bbl/day]	Inhibitor Concentration GPT	Predicted Pressure [psi]
700	0	1296
700	0.2	933
700	0.6	933

Source: Own elaboration.

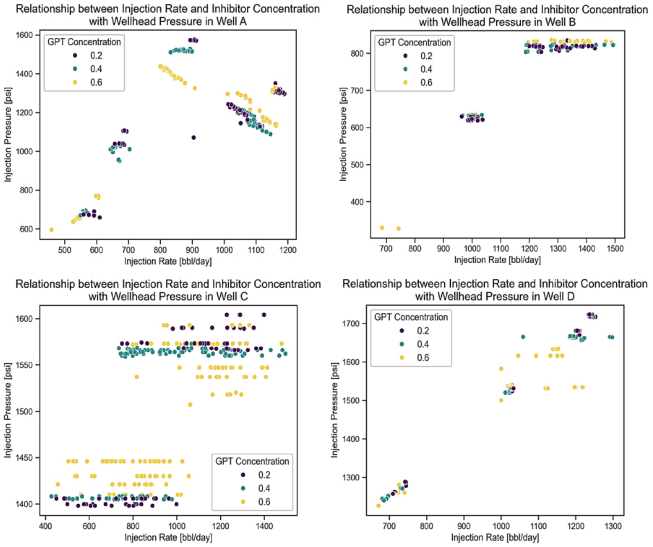

Figure 12. Scatter plot of pressure data considering its relationship with the injection rate and inhibitor concentration in the evaluated wells.
Source: Own elaboration.

Table 12.
Prediction of Injector Well C's injection rate based on operating pressure and different commercial inhibitor concentrations.

Injection Rate [bbl/day]	Inhibitor Concentration GPT	Predicted Pressure [psi]
700	0	1296
700	0.2	933
700	0.6	933

Source: Own elaboration.

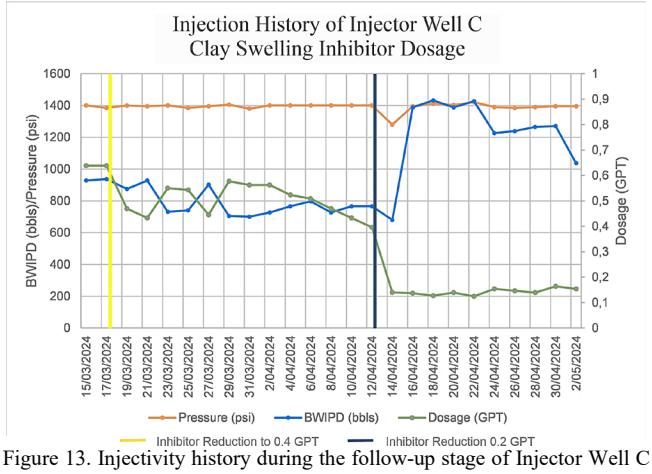

Figure 13. Injectivity history during the follow-up stage of Injector Well C vs. inhibitor concentration.
Source: Own elaboration.

Scatter plots in Fig. 12, show that inhibitor concentration does not affect injectivity in Injector Well B. In Injector Well C, two pressure behaviors are observed: pressure remains constant for injection rates below or near 1000 BWIPD, while at higher rates, pressure increases.

Increasing inhibitor concentration to 6 GPT raises pressure at low rates but reduces it at higher rates. Similarly, in Injector Well D, inhibitor concentration has no effect

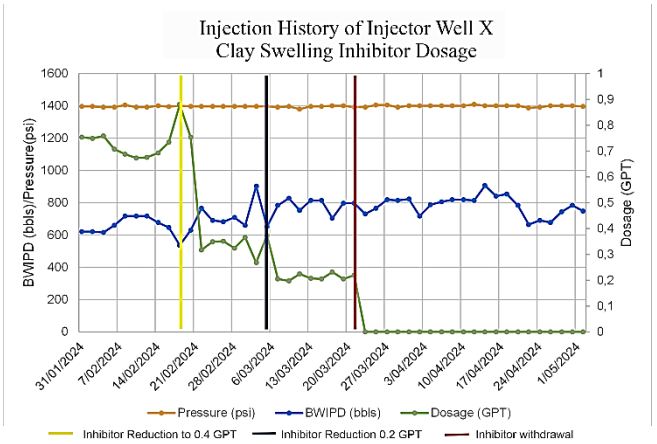

Figure 14. Injectivity history during the monitoring stage of Injector Well X vs. clay swelling inhibitor concentration.
Source: Own elaboration.

below 1000 BWIPD, but at higher pressures, 6 GPT reduces injection pressure. An injection rate prediction was performed for an operating pressure of 1400 psi, which is the controlled variable in Injector Wells C and D.

As shown in Table 12, results indicate that injection rates do not exceed 1000 BWIPD for any inhibitor concentration, with predicted values close to 700 BWIPD at 1400 psi.

4.2 Field Evaluation Follow-Up

A subsequent long-term evaluation of the field's injection wells demonstrated that reducing the inhibitor concentration (Fig. 13) or even eliminating it (Fig. 14) does not significantly affect well injectivity.

This follow-up confirmed that injectivity remains stable without the need for high inhibitor levels, suggesting that the inhibitor's presence is not critical for the continuous performance of injection wells. These findings highlight the feasibility of operational management without relying on inhibitors, enabling cost optimization. In summary, the follow-up phase confirmed the low sensitivity of the inhibitor to injectivity changes and emphasized the viability of operating wells with minimal or no inhibitor concentration without compromising injection efficiency.

5 Conclusions

Once the field test was conducted, it was confirmed that the laboratory results were consistent and that by analyzing the instantaneous variation of injection rates, the sensitivity of the inhibitor to pressure changes in the injection wells could be observed.

The results demonstrate that it is feasible to perform an instantaneous evaluation of the rate-pressure relationship in water injection wells based on the use and/or concentration of the commercial swelling-hydration inhibitor. This suggests that it is possible to operate the wells at lower inhibitor concentrations or even eliminate its dosing in some wells where it does not significantly improve

injectivity, especially at low injection rates. This optimization can lead to significant economic savings and improve the injection performance of the reservoir.

Additionally, some instantaneous pressure increases in the wells may be related to variations in the mechanical conditions of the injection system rather than formation-level plugging, highlighting the importance of strict control over operational conditions.

The field methodology implemented to evaluate the influence of the swelling-hydration inhibitor proved effective in establishing cost-effective injectivity scenarios. This provides a solid basis for well-informed technical decisions to enhance economic efficiency by optimizing inhibitor dosing according to each well's specific needs.

Importantly, this methodology is applicable across different lithological sequences and sample types—both consolidated core samples and fragmented trench samples—since it focuses on identifying clay minerals prone to swelling and hydration in depleted reservoirs where injectivity decline is observed. By detecting minerals with swelling potential, this approach can be applied preventively or correctively in any water injection well where produced water is injected, regardless of the mineralogical arrangement in the rock matrix. Thus, it offers a versatile tool for evaluating and managing clay-related formation damage in a broad range of field conditions.

References

[1] Abbas, A., Flori, R., AL-Anssari, A., and Alsaba, M., Laboratory analysis to assess shale stability for the Zubair Formation, Southtern Iraq. Journal of Natural Gas Science and Engineering 56, pp. 315-323, 2018. DOI: https://doi.org/10.1016/j.jngse.2018.05.041

[2] Abbasi, S., Shahrabadi, A., and Golghanddashti, H., Experimental investigation of clay mineral effects on the permeability. Society of Petroleum Engineers, Art. 4248, 2011. DOI: https://doi.org/10.2118/144248-MS

[3] Alsaba, M., Al-Marshad, A., Abbas, A., Abdulkareem, T., Al-Shammary, A., Al-Ajmi, M., and Kebeish, E., Laboratory evaluation to assess the effectiveness of inhibitive nano-water-based drilling fluids for Zubair shale formation. Journal of Petroleum Exploration and Production Technology 10, pp. 419-428, 2019. DOI: https://doi.org/10.1007/s13202-019-0737-3

[4] Anderson, R., Ratcliffe, I., Greenwell, H., Williams, P., Cliffe, S., and Coveney, P., Clay swelling a challenge in the oilfield. Earth-Science Reviews, 98(3-4), pp. 201–216, 2010. DOI: https://doi.org/10.1016/j.earscirev.2009.11.003

[5] API Methylene blue test for drill solids and commercial bentonites. Section 12 in: API RP 13I: Laboratory Testing of Drilling Fluids, 7th ed., ISO 10416:2002. American Petroleum Institute, 2004.

[6] API 1998 Porosity determination and permeability determination. sections 5 and 6 in: API RP 40: Core Analysis, 2nd ed., American Petroleum Institute, 1998.

[7] Balaban, R.C., Ferreira, E., and Rodrigues, M., Design of experiments to evaluate clay swelling inhibition by different combinations of organic compounds and inorganic salts for application in water base drilling fluids. Applied Clay Science, pp. 124-130, 2015. DOI: https://doi.org/10.1016/j.clay.2014.12.029

[8] Bailey, L., Keall, M., Audibert, A., and Lecourtier, J., Effect of clay/polymer interactions on shale stabilization during drilling. IFP Langmuir 10, pp. 1544-1549, 1994. DOI: https://doi.org/10.1021/la00017a037

[9] Bishop, S.R., The experimental investigation of formation damage due to the induced flocculation of clays within a sandstone pore structure by a high salinity brines. Paper presented at the SPE European Formation Damage Conference, The Hague, Netherlands, June 1997. DOI: https://doi.org/10.2118/38156-MS

[10] Cheng, K., and Heidari, Z., A new method for quantifying cation exchange capacity in clay minerals. Applied Clay Science 161, pp. 444-455, 2018. DOI: https://doi.org/10.1016/j.clay.2018.05.006

[11] Civan, F., Reservoir formation damage: fundamentals, modeling, assessment, and mitigation, 1st ed., Gulf Publishing Company, Houston, Texas, USA, 2000. DOI: https://doi.org/10.1016/C2020-0-03547-4

[12] Ecopetrol., Reporte integrado de gestión sostenible [online]. 2015. Bogotá. Available at: https://www.ecopetrol.com.co/wps/portal/Home/es/ResponsabilidadEtiqueta/InformesGestionSostenibilidad/Informesdegestion

[13] Fink, J.K., Hydraulic fracturing chemicals and fluids technology. Gulf Professional Publishing, Oxford, UK, 2013. DOI: https://doi.org/10.1016/C2012-0-02544-6

[14] Instituto de Hidrología, Meteorología y Estudios Ambientales (IDEAM), [online]. 2015. Estudio Nacional del Agua 2014. Bogotá. Available at: https://www.ideam.gov.co/sala-de-prensa/informes/Estudios%20nacionales%20del%20agua

[15] Karpinski, B., and Szkodo, M., Clay minerals mineralogy and phenomenon of clay swelling in oil and gas industry. Advances in Materials Science, 15(1) pp. 37-55, 2015. DOI: https://doi.org/10.1515/adms-2015-0006

[16] Laird, D.A., Influence of layer charge on swelling of smectites. Appl. Clay Sci. 34, pp. 74-87, 2006. DOI: https://doi.org/10.1016/j.clay.2006.01.009

[17] Leone, J.A., and Scott, E.M., Characterization and control of formation damage during waterflooding of a high-clay-content reservoir. Society of Petroleum Engineers - SPE Res Eng, 3(4), pp. 1279–1286, 1988. DOI: https://doi.org/10.2118/16234-PA

[18] Liu, S., Mo, X., Zhang, C., Sun, D., and Mu, C., Swelling inhibition by polyglycols in montmorillonite dispersions. Journal of Dispersion Science and Technology 25, pp. 63–66, 2004. DOI: https://doi.org/10.1081/DIS-120027669

[19] Kleven, R., and Alstad, J., Interaction of Alkali, Alkaline-Earth and Sulphate Ions with clay minerals and sedimentary rocks. Journal of Petroleum Science and Engineering, 15(1996), pp. 181-200, 1996. DOI: https://doi.org/10.1016/0920-4105(95)00085-2

[20] Norrish, K., The swelling of Montmorillonite, Discussions Faraday Soc., 18, pp. 120-134, 1954. DOI: https://doi.org/10.1039/DF9541800120

[21] Ramos, N., Cabrera, M., Liberti, I., Cevasco, C., Dibilio, J., Belén, M., y Renta, D., Utilización de ensayos de expansión de arcillas para el análisis de inhibidores en la cuenca del Golfo San Jorge, [online], 2017. Available at: https://www.researchgate.net/publication/318040185_utilizacion_de_ensayos_de_expasion_de_arcillas_para_el_analisis_de_inhibidores

[22] Sarkisyan, S.G., Origin of authigenic clay minerals and their significance in petroleum geology. Sedimentary Geology, 7, pp. 1-22, 1972. DOI: https://doi.org/10.1016/0037-0738(72)90050-4

[23] Valle Medio del Magdalena—Agencia Nacional de Hidrocarburos. [online], 2024. Available at: https://www.anh.gov.co/es/hidrocarburos/oportunidades-disponibles/procesosde-seleccion/ronda-colombia-2010/tipo-1/valle-medio-del-magdalena/

[24] Yang, R., Zhang, J., Chen, H., Jiang, R., Sun, Z., and Rui, Z., The injectivity variation prediction model for water flooding oilfields sustainable development. Energy, 189, Art. 116317, 2019. DOI: https://doi.org/10.1016/j.energy.2019.116317

[25] Zhou, Z., Gunter, W.D., Kadatz, B., and Cameron, S., Effect of clay swelling on reservoir quality. Petroleum Society of Canada, art. 96-07-02, 1996. DOI: https://doi.org/10.2118/96-07-02

[26] Zhou, Z.J., Cameron, S., Kadatz, B., and Gunter, W.D., Clay swelling diagrams: their applications in formation damage control. Paper presented at the SPE Formation Damage Control Symposium, Lafayette, Louisiana, February, 1996. DOI: https://doi.org/10.2118/31123-MS

J.A. Peña-Mateus, received the BSc. Eng in Petroleum Engineering in 2021, the MSc. in Hydrocarbon Engineering in 2024, both from the Universidad Industrial de Santander (UIS), Bucaramanga, Colombia, where her studies focused on geomechanics and molecular dynamics. Between 2023 and 2024, she worked for the Laboratorio de Diagnóstico de Pozo, Escuela de Ingeniería de Petróleos, UIS. Currently, she is involved in energy transition projects at UIS, with a focus on geothermal energy, including topics such as geothermal well integrity, estimation of geothermal gradient, heat flow, and electric power potential based on data from the oil and gas industry.
ORCID: 0009-0004-5182-308X

M.P. Mosquera-González, recived the BSc. Eng in Chemical Engineering in 2018 from the Industrial University of Santander (UIS), Colombia. She currently works as a service and laboratory professional at the Well Diagnostics Laboratory, affiliated with the School of Petroleum Engineering. Her research interests include formation damage and reservoir engineering.
ORCID: 0009-0009-6232-707X

F.I. Archer-Martínez, received the BSc. Eng in Petroleum Engineering in 2004 from the Universidad Central de Venezuela, and the MSc. in Petroleum Engineering in 2011 from the IFP School, Rueil-Malmaison, France. From 2004, he worked for consulting companies within the power and O&G sector. Nowadays, he is Chief Operating Officer (COO) y Co-Founder of Bonpland Energy y Chief Executive Officer (CEO) of EOR Wave S.A.S. His research interests include chemical enhanced/improve oil recovery, well stimulation, and numerical reservoir simulation.
ORCID: 0009-0003-3670-064X

E.A. Gómez-Cepeda, received the BSc. Eng in Petroleum Engineering in 2016, and the MSc. in Hydrocarbon Engineering in 2020, all of them from the Universidad Industrial de Santander, Bucaramanga, Colombia. From 2023, he has worked as Extension Laboratories Coordinator of the School of Petroleum Engineering for Universidad Industrial de Santander. Nowadays, he is Chief Executive Officer (CEO) of LOGOZ SAS. His research interests include chemical enhanced/improve oil recovery, reservoir engineering, well stimulation, and numerical reservoir simulation.
ORCID: 0000-0002-4580-3654

Y. Jaimes-Barajas, received the BSc. and MSc. in Chemistry from Universidad Industrial de Santander, Bucaramanga, Colombia. She has worked at Occidental de Colombia since 2004, holding roles such as Laboratory Supervisor, Facilities Engineer, and currently Mechanical Integrity Engineer. Her experience includes produced water treatment, asset integrity, corrosion control, crude measurement, environmental compliance, and risk management in oil and gas operations.
ORCID: 0009-0005-8786-5510